ENGINEERING TRANSACTIONS • *Engng. Trans.* • **65**, 3, 447–460, 2017
Polish Academy of Sciences • Institute of Fundamental Technological Research (IPPT PAN)
National Engineering School of Metz (ENIM) • Poznan University of Technology

Research Paper

Design of a Rice Rope Laying Machine for Direct Sowing

Xiao-Lian LV[1)], Xiao-Rong LV[2)*], Rong-Chao MA[2)]

[1)] *College of Machinery & Electronic Engineering*
Chuzhou University
Anhui, China

[2)] *College of Mechanical & Electrical Engineering*
Sichuan Agricultural University
Yaan, China
*e-mail: Lxrxj2008@163.com

The research and development of a rice rope laying machine (RRLM) provides new ideas for a design of a rice direct seeding machine, and solves existing problems encountered in direct seeding techniques currently in use. The RRLM has been developed based on an in-depth analysis of the design principles and main structure parameters of rice direct seeding machines. The completed machine consists of all necessary components including an anti-blocking device, sowing device, opening device, banking device, compacting device, etc. The optimal design of the parts and structure of the RRLM was completed using the three-dimensional Unigraphics NX (UG NX) software. The rationale and the performance of the machine and its components were analyzed using this virtual prototyping technology. The key technology problems commonly encountered, which included the opener being easily plugged up, the difficulty in adjusting/controlling the number of seeds per hole, and seeding rope easily broking during the process of laying, have all been effectively solved. The field test results have shown that this machine has the advantage of good maneuverability and high working efficiency, the reliability and quality of seeding rope placement meets (fulfills) the design requirements, the profiling and compacting effect of the machine is very good, and the uniformity of seeding depth and accurate rope placement are guaranteed.

Key words: rice rope laying machine (RRLM), optimal design, research and development, virtual design, structure analysis, performance test.

1. Introduction

The development of rice planting mechanization depends primarily on the development of rice cultivation technology. Economically developed countries have achieved a single mechanized mode for planting cropping patterns. In the United States, Australia and Italy, direct seeding mechanization is being used.

In Japan and South Korea, mainly mechanized transplanting of rice seedlings is used. In China, different mechanized models have been developed, because of the vast rice cropping region and various corresponding cropping systems [1].

The technology of rice direct seeding is characterized by high efficiency, low labor intensity, simple operating machinery, low operation costs, high yield, and being suitable for large-scale operation. Nevertheless, the overall price can be high with strict requirements associated with rice variety, growth stage, irrigation conditions, soil preparation quality and weed control technology as well as the need of handling a larger quantity of seeds. Therefore, it is very difficult to promote such technology in China. Presently, in China, most rice direct sowing machines are re-structured from wheat planter machines. Such machines are complex, bulky, and costly, consume much energy, and have a large turning radius. In addition, the opener device gets easily plugged up, the ditching depth is unstable, the seed spacing is inaccurate and the number of seeds per hole is difficult to adjust [2, 3]. Therefore, according to the actual situation of the rural areas, there is an urgent need to solve these problems so that RRLMs can be produced to meet farmers' requirements in accordance with their actual purchasing ability. This study focuses on using RRLMs to solve these problems of the rice direct sowing machine before actual production. This is a research field that has a potential, value and significance.

2. Overall structural framework design

2.1. Design objectives and requirements

Based on the RRLM seeding requirements and seeding technology studied at home and abroad [4–6], the RRLM design goals are: light weight, low speed, the seed rope disk turning by rope friction when driving, the rotating tube and guide-line wheel rotating without driving, good sowing performance, and simple structure. Additionally, the machine can be used in the field or in a greenhouse as well, to meet the needs of different kinds of seed rope sowing.

2.2. Structure and working principle

The overall structure design of RRLM is shown in Fig. 1. The machine's main components include traction (marking) device, anti-blocking device (device for clearing the debris, straw etc. by moving them to each side of the cleared area), opening (furrowing) device, rice rope sowing device, banking device, compacting device, and so on. The RRLM works by being pulled by a tractor, using the tractor's traction movement. At the same time, the end of the rope is first fixed to the earth, and the tractor pulls the prototype forward. The anti-blocking device is installed in front of the opener, to launch straw and other debris out

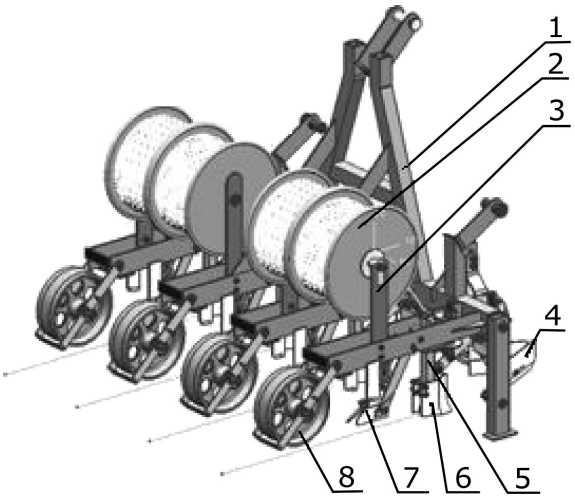

Fig. 1. Structure of the RRLM: 1 – rack, 2 – seeding rope disc, 3 – seeding rope disc seat, 4 – anti-blocking device, 5 – sowing device, 6 – opening device, 7 – banking device, 8 – compacting wheel.

of the seed bed to prevent plugging of the opener. When the machine moves forward, the anti-blocking boards push rice stubble and other debris out of the sowing belt way, The furrowing device makes the seed furrow that is 4–6 cm deep, the rope-type seeding mechanism lays the seed rope on the fields smoothly, the banking device pushes soil into the seed rope ditch and thus covers the seed rope while the compacting device then compacts the soil. Therefore, the RRLM completes the cycle of furrowing, laying seeding rope, banking and compacting all at once.

3. The design of key working components

Virtual design technology provides a product design environment, optimizes the product design process, and provides strong support for the research and development of new products. During the first stage, the virtual simulation technology can greatly improve and predict potential problems arising in the design process, and improve design quality, therefore reducing design errors and production costs. In China, the application of the virtual prototyping technology application has been directed towards the field of agriculture, especially for agricultural engineering, and is considered a necessary measure for engineering design and production. The RRLM's structural scheme, main technical parameters, and each part and component's functional requirements and features have all been optimally designed with the virtual design software.

3.1. Suspension device design

3.1.1. The suspension device structural design. To improve the versatility and utilize power machinery, the RRLM adopts the hanging mode from a tractor. The location of the suspension and force balance will affect the penetrating performance and working stability of the furrower.

In Fig. 2, G is gravity, P is the traction force, R is the soil resistance (including vertical supporting force and the friction of the ditch to the opener), S is the force of gravity G, and resistance R. When the force S and the traction P work in line and they are in a state of the balance, as shown in Fig. 2a, the opener keeps the trench depth unchanged and stable. When the elevation angle α (the angle between the traction and the horizontal direction) is greater, as shown in Fig. 2b, the pressure of the opener's front portion is smaller on the ditch, and its penetration is shallower; or when the elevation angle is smaller, the penetration is deeper. Thus, changing the position of the ditching traction point O changes its penetration depth. As shown in Fig. 2c, when point O is in a lower or more forward position, the force S and traction P provide the torque pushing the opener downward, so the opener penetrating depth is increased or opposite situation takes place the depth decreases, as shown in Fig. 2d. In order to obtain the best traction stability with the smallest traction force, the traction

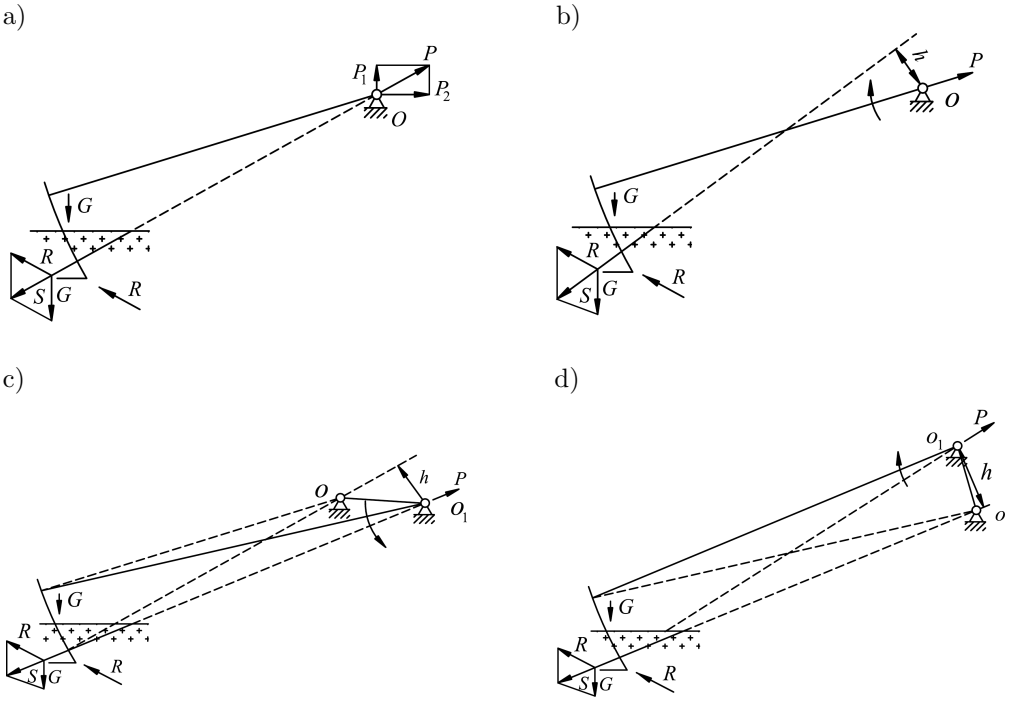

FIG. 2. Hanging position and force.

line position is very important. The hanging and traction points in the design of the level of the size and the elevation angle were determined by calculating the force system equilibrium conditions. The above analysis results are shown in Table 1.

Table 1. The relationship between the depth of furrow opener and traction position.

Position relationship of S (resultant force) and P (traction force)	α (elevation angle)	O (furrower traction point)	H (buried depth opener)
Force in a straight line	Constant	Constant	Constant
Force not in a straight line	Increase	Constant	Decrease
Force not in a straight line	Decrease	Constant	Increase
Force not in a straight line	Constant	Forward or lower	Increase
Force not in a straight line	Constant	Backward or higher	Decrease

3.1.2. The suspension device strength check. In order to determine whether the strength of the suspension device meets the design demands, the finite element, three-dimensional analysis model was implemented using UG NX [7]. The three-dimensional model has been appropriately simplified by removing those characteristics of little effect on the analysis results, such as some chamfers, etc. This reduces the degree of complexity of meshing the finite element model and accelerates the completion speed of the finite element analysis. Meanwhile, more dense grids were arranged in the region of stress concentration of the suspension device, while the relatively sparse grids were arranged in the gently changing stress region of the suspension device. The finite element model of the suspension device is shown in Fig. 3.

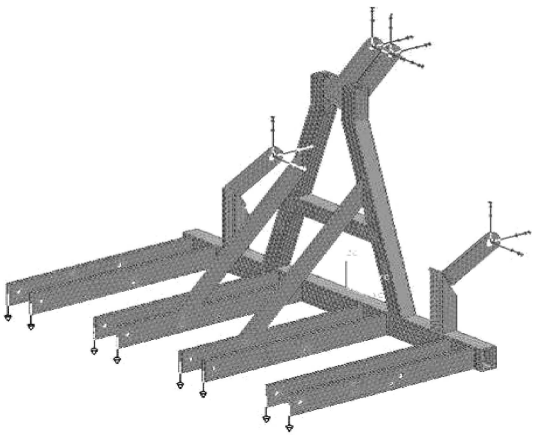

FIG. 3. 3D model and finite element model of the suspension device.

The analysis results showed that when the suspension device load is 113 N, the minimum equivalent stress is $3.99 \cdot 10^{-2}$ N/mm^2, and the maximum equivalent stress is 0.5125 N/mm^2. The material of suspension device is carbon structural steel, please see the tables in [8], and the yield strength is $\sigma_s = 235$ N/mm^2

$$\gamma_n = \frac{\sigma_s}{\sigma_{\max}}, \tag{3.1}$$

where γ_n – the safety coefficient, σ_s – the yield strength of the material, and $\sigma_{\max}$ – the maximum equivalent stress.

From the formula (3.1) can be obtained: $\gamma_0 = \frac{235}{51.25} = 4.59$. The safety coefficient of the suspension device is large enough in the maximum stress, showing that it has sufficient stability and strength according to the theoretical static strength analysis.

3.2. Anti-blocking device design

The anti-blocking device performance is one of the key performance indicators of the machine. The anti-blocking device includes an anti-blocking board, side board, spring, orientation axis and intermediate axis, as shown in Fig. 4.

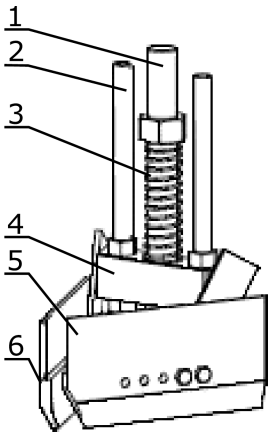

FIG. 4. Anti-blocking device: 1 – intermediate axis, 2 – orientation axis, 3 – spring, 4 – side board, 5 – right anti-blocking panel , 6 – left anti-blocking panel.

When the machine works the anti-blocking boards 5 and 6 push debris from the sowing belt center to its' two sides. The anti-blocking device is joined to the anti-blocking box on the rack via the intermediate axis and the nuts. The vertical position from the ground of the anti-blocking device is then adjusted by using the nuts' adjustment. When it encounters an obstacle, the anti-blocking device lifts to avoid being damaged by hard objects. After the device passes

over the obstacle, it returns to its original position, relying on its own weight and spring tension. The anti-blocking device is working to make the roots or clods slip out along the edge of the anti-blocking board, i.e., the debris is guided outside the seed furrow. In the xOy plane, the external forces on the debris R must be guaranteed in the friction cone outside, as the friction cone forms the interaction between the board surface and debris as shown in Fig. 5. If a clod located at point M slips to the board end along the tangential edge, the formula (3.2) must be satisfied by the analysis

$$\left.\begin{aligned} N &= R\sin\phi \\ F_f &\le R\cos\phi \\ F_f &= N\tan\phi \end{aligned}\right\}, \tag{3.2}$$

where R is the force of the external action on the clod, and F_f is the friction of the board surface to debris, N is the positive pressure of the plate face to debris.

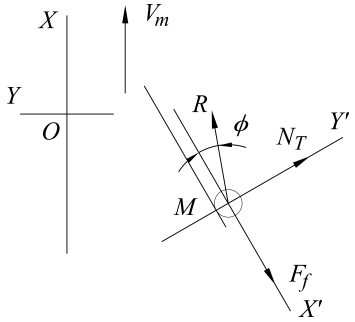

FIG. 5. The condition of cover of anti-blocking mechanism.

The angle α_m is between the line through point M point and forward direction, so $\tan\phi \times \tan\alpha_m \le 1$ can be obtained.

Because

$$\tan(\phi+\alpha_m) = \frac{\tan\alpha_m + \tan\phi}{1 - \tan\alpha_m \times \tan\phi} \ge 0,$$

while these values of $\tan\alpha$ and $\tan\phi$ are all greater than zero, $0 < \alpha_m + \phi \le 90^\circ$ can be obtained. Therefore, the guide debris conditions of the anti-blocking device can be obtained.

The guide debris conditions are

$$0 < \alpha_m < 90^\circ - \phi, \tag{3.3}$$

where α_m is the angle between the anti-blocking device and the forward direction and ϕ is the friction angle.

3.3. Sowing device design

The sowing device is the core part of the RRLM. The sowing device mainly includes: the guide-line axle, guide-line wheel, guide-line body, rotating tube axis, rotating tube, etc., as shown in Fig. 6.

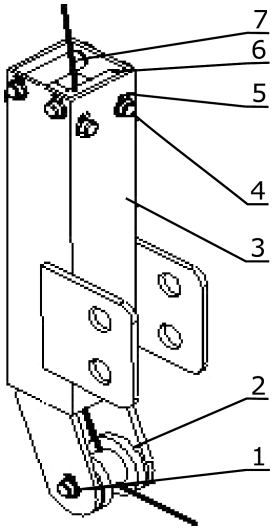

FIG. 6. The structure of the seed rope laying device: 1 – guide-line wheel axis, 2 – guide-line wheel, 3 – guide-line body, 4 – rotating tube axis, 5 – ring, 6 – rotating tube, 7 – seed rope.

The rotating tube and guide-line wheel are the two main parts of the device. The diameter of the rotating tubes is 6 mm and the length is 18 mm by analysis [9]. The rotating tubes are installed in the upper part of the sowing device. A guide-line wheel is mounted on the lower portion of the sowing device, and its main role is to guide seed rope into the seed furrow. The device features that seed rope 7 is vertically conveyed to guide-line wheel 2 by the rotating tube 6, at that level the seed rope is then conveyed into the seed furrow by the guide-line wheel. In the process of transmission, the upper conveying seed rope uses the rolling structure, and the lower turning point of maximum friction is absorbed by the light bearing structure. To make the designed rope sowing system work smoothly, and prevent the seed rope from being broken, the sowing rope performance was determined using force analysis, as shown in Fig. 7. Because the friction and support force of the seed rope is a pair of action and re-action forces, the same as the friction and support force of the rotating tube under the rope drive, the force balance equation of the seed rope is as follows:

$$\left.\begin{aligned} F_1\cos\theta + F_2\cos\theta &= F_{R2}\cos\phi \\ F_1\sin\theta_+ F_{R2}\sin\phi &= F_2\sin\theta \end{aligned}\right\}. \tag{3.4}$$

F_2 can be obtained:

$$F_2 = \frac{F_1(\sin\theta + \cos\theta\tan\phi)}{\sin\theta - \cos\theta\tan\phi} = \frac{F_1(\sin\theta + f_{v1}\cos\theta)}{\sin\theta - f_{v1}\cos\theta}. \tag{3.5}$$

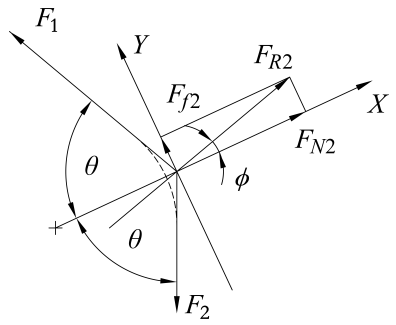

FIG. 7. The force analysis of seed rope.

In rope tension testing [10], F_1 is the force needed to pull the rope wheel, and it measures $F_1 < 0.5$ N. So by introducing $F_1 < 0.5$ N into Eq. (3.5) we obtain:

$$F_2 = \frac{F_1(\sin\theta + f_{v1}\cos\theta)}{\sin\theta - f_{v1}\cos\theta} < \frac{0.5(\sin\theta + f_{v1}\cos\theta)}{\sin\theta - f_{v1}\cos\theta}. \tag{3.6}$$

In this formula, F_2 is the covalent force to pull the rope wheel and rotating tube, it can be obtained as $F_2 < 0.68$ N by the derivation analysis, while similarly the tension of the seed rope at the guide-line wheel is $F_3 < 0.92$ N. The analysis shows that the maximum pulling force of the seed rope from the rope disk to seed ditch is 0.92 N, which is far less than the maximum allowable tension. Sowing of the seed rope can be performed by its own friction without any external driving forces.

4. Prototype virtual detection and processing

Virtual prototype simulation was performed using UG NX software. The RRLM was studied as to the coordination and functionality of the moving parts, and inspected to see whether any interference will occur during the movement process, and checked to see whether the work process can achieve the desired effect [10–13]. Through the quality analysis of the RRLM it is known that the whole weight is 106 kg, due to virtual assembly bolts, etc. being omitted, the virtual machine weight is lighter than the actual weight, centric coordinates are $(-0.05, -228.31, -44.72)$, the x direction is along the machine's center, the

y direction is near the opener back, the z direction is less than 44 mm from the upper surface of the crossbeam. The center of gravity was somewhat partially behind and higher by the machine analysis. On this basis, the corresponding adjustment on structure and size of the prototype were made. Using an increased counterweight, the center of gravity was then adjusted to the center position.

On the basis of a virtual three-dimensional model design analysis, the prototype processing was conducted, and the completed manufactured prototype is shown in Fig. 8.

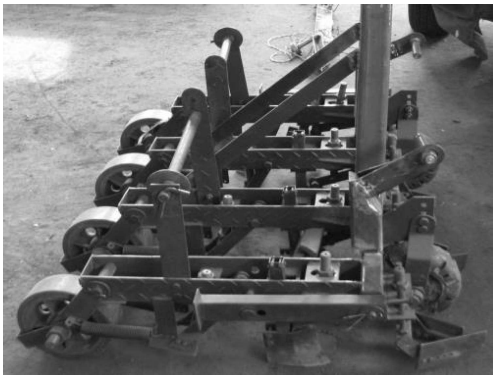

FIG. 8. Prototype of the RRLM.

5. Testing and result analysis

5.1. Testing objective, content and condition

Field testing objectiveŁşThe testing objective was to observe the RRLM's adaptability in the field, its structural reliability, the functionality of the overall configuration, determining the performance parameters of the working parts, and checking whether the prototype meets the design requirements. The other objective was to check the working performance and quality of the machine, and whether it meets the requirements of agricultural technology.

Testing content in field: The testing contents were: the working reliability and stability of the prototype, its adaptability, anti-blocking performance, performance in the field, and the penetrating performance of the prototype in different ground conditions as well as the overall structural soundness of the prototype.

Testing conditions: The soil types were brown loam. At 0–5 cm depth, the soil's average water content was 18.06%, and the soil's bulk density was 0.93 g/cm^3. After a laser grader inspected the ground to confirm a smooth surface, without large clods, the standard deviation of surface roughness was not more than 3 cm.

5.2. Testing the anti-blocking device

The effect of main structural parameters on performance was tested for the anti-blocking device. The main function of the anti-blocking board is to clear by pushing away debris, straw, clods, etc., the anti-blocking board is designed as shown in Fig. 9a, and the anti-blocking device for testing is shown in Fig. 9b.

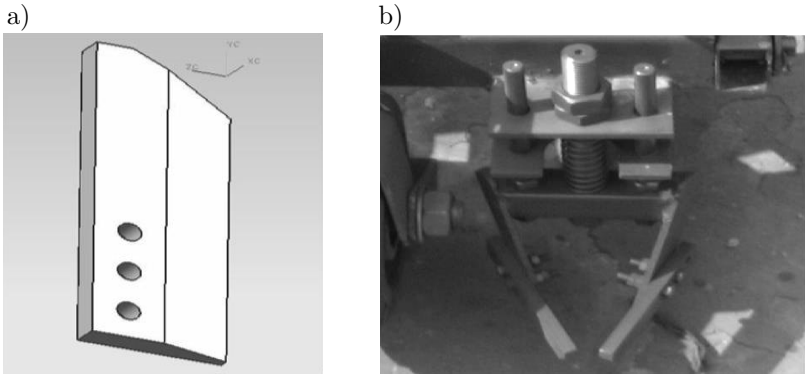

FIG. 9. The testing of the anti-blocking board and the anti-blocking device: a) the anti-blocking board, b) the anti-blocking device.

The test results showed that the designed anti-blocking device has a significantly smooth and anti-blocking effect on the seedbed. Without the anti-blocking device, there were a lot of straw and clods in the front of the opener, and the soil easily accumulated causing it to become blocked and fail, as shown in Fig. 10a. After the anti-blocking device was installed, the seedbed was relatively flat, smooth, and with less straw, rice stubble and clods, as shown in Fig. 10b.

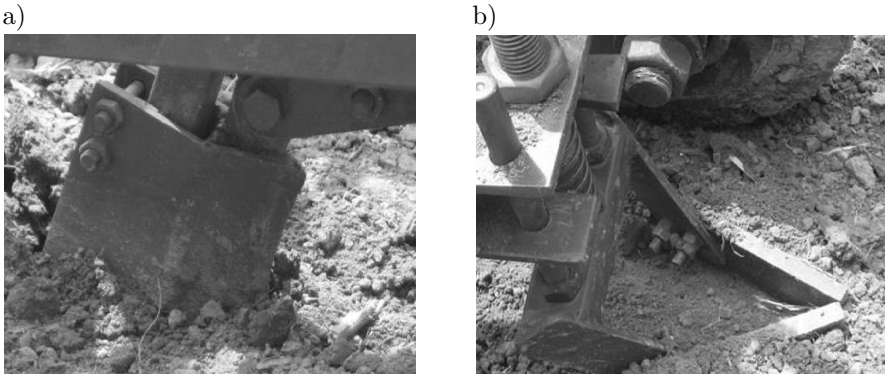

FIG. 10. The actual situation on the surface of the seedbed: a) seedbed without anti-blocking device, b) seedbed with anti-blocking device.

While a lot of clods, rice stubble, straw and other debris accumulated on both sides of the sowing belt the testing showed that the designed anti-blocking device can push the debris out of the sowing belt way under most conditions and the working conditions of the opener were greatly improved.

5.3. Compacting wheel slip ratio measurements

Measurement method [14]: during the sowing process, the number of turning cycles per each wheel was recorded and the actual walking distance was measured. The compacting wheel radius is 200 mm; each wheel was measured five times to obtain the average value.

Slip ratio calculation formula is

$$\eta = \frac{S_1 - S_2}{S_1} \times 100\%, \tag{5.1}$$

where η – slip rate of compacting wheel, S_1 – compacting wheel theoretical walking distance, $S_1 = 2\pi r \cdot n$ [cm], S_2 – compacting wheel actual walking distance [cm], γ – compacting wheel radius [cm], n – compacting wheel turning circle number.

Measured data and calculated results are shown in Table 2. The operating speed was 0.44 km/h and the average slip rates were 4.44% for wheel 1, 5.58% for wheel 2, 7.81% for wheel 3, 6.96% for wheel 4, and they all meet the planting requirements.

Table 2. Slip ratio measurements and results for compacting wheel.

The actual walking distance [cm]	Wheels turning circle 10			Wheels turning circle 18		Slip ratio, η
	1	2	3	4	5	
Wheel 1	635	641	650	1181	1203	4.44%
Wheel 2	651	659	638	1203	1196	5.58%
Wheel 3	644	680	649	1216	1243	7.81%
Wheel 4	649	666	652	1215	1222	6.96%

5.4. Planting depth determination

Measurement method: five sowing belts were selected randomly, and five points were selected for each sowing belt; then, a reference point was selected, and the soil around the seed rope was poked, and the sowing depth was measured with a ruler. Measured data, and calculated results are shown as Table 3.

Testing showed that the average sowing depth was 29.72 mm, the average standard deviation was 1.9, the average coefficient of variation of sowing depth

Table 3. Coefficient of variability of planting depth.

Row	Sowing depth [mm]					Mean [mm]	Standard deviation	Coefficient of variation
	A	B	C	D	E			
1	26.0	29.8	29.5	30.5	31.6	29.48	2.11	7.16
2	29.4	31.0	29.8	27.5	30.1	29.56	1.29	4.36
3	29.7	31.2	28.2	32.5	28.0	29.92	1.94	6.48
4	32.1	33.3	31.3	29.5	26.7	30.58	2.57	8.40
5	30.7	29.0	30.0	26.5	29.2	29.08	1.59	5.55
Average						29.72	1.90	6.39

was 6.39%, and the largest coefficient of variation was 8.40%. These results show that the machine seeding depth is uniform and fulfills to the basic requirements of the "grain seeder grading standards of product quality".

6. Conclusions

1) The designed and developed rice rope laying machine is structurally simple and compact, and it can effectively solve the problems of the opener blocking, inaccurate sowing distance, and the difficulty in adjusting of the number of seed per hole. The machine has numerous advantages. It works reliably and not only creates good bed conditions conducive to seed sprouting with less soil disturbed, but has low power consumption, strong ability in the field and many other advantages.
2) Using UG NX software suspension frame a three-dimensional model was established to carry out the finite element analysis. The suspension weak link was identified at the middle beam root and the beam welding area. This is consistent with the problem of middle hanging beam deformation and collapse during practical application. Through the testing, the problem was corrected and the optimum suspension structure was ultimately determined and employed.
3) The designed anti-blocking device has a clearance rate of more than 90%, only leveling the planting belt. This not only reduces the machine's power consumption, but also provides good bed conditions for seed growth.
4) The seed rope disc rotates smoothly and the rope sowing effect is excellent. There is little rope breakage when working. Testing proved that the innovative idea of the designed rotating sowing seed rope is feasible and the designed sowing device achieves reliable work performance.

Acknowledgment

This study was supported by the National Natural Science Foundation of China (50775150).

References

1. Chen W.S., *Rice direct seeding status, problems and countermeasures*, Anhui Agricultural Science Bulletin, **4**: 44–45, 2011.
2. Luo X., Xie F., Ou Y., Li B., Zheng D., *Experimental investigation of different transplanting methods in paddy production*, Trans. Chin. Soc. Agr. Eng., **20**(1): 136–139, 2014.
3. Lv X.R., Ren W.T., Lv X.L., *Analysis and research for the technology of rice direct sowing with seed rope*, J. Agr. Mech. Res., **1**: 212–215, 2008.
4. Ren W.T., Li X.S., *Effect of the technique of rice direct sowing with seeds twisted in paper rope on rice yield character*, J. Shenyang Agr. U., **36**(3): 265–270, 2013.
5. Hiyoshi K.J, Nagata M., Umezaki T., Tadeo B.D., Wang H., *Basic study on rice transplanted in the mulching cultivation system for early season culture rice*, J. Jap. Soc. Agr. Mach., **60**(4): 13–22, 1998.
6. Tsuno K., Umezaki T., *Effects of used-paper mulching on growth of early-season culture rice*, Jpn. J. Crop. Sci., **67**(2): 143–149, 1998.
7. Zhang L.H., Lv X.R., *UG NX 9.0 computer-aided design and manufacture of practical course*, Beijing University Press, Beijing, 2015.
8. Li L.J., *Machine Design*, Higher Education Press, Beijing, 2013.
9. Lv X.R., Lv X.L., Ren W.T., *Research and development of the rice rope direct seeding machine*, J. Nanjing Agric. Univ., **33**(3): 104–108, 2011.
10. Hong R.J., *Advanced simulation training*, Qinghua University Press, Beijing, 2015.
11. Fabio B., Francesco C., Li K., Milite A., Muzzupappa M., *Dynamic simulation of virtual prototypes in immersive environment*, Int. J. Adv. Manuf. Technol., **43**(5–6): 620–630, 2009.
12. Emad A.M., Rawabdeh I., *An application of finite element method and design of experiment in the optimization of sheet metal blanking process*, Jordan J. Mech. Indust. Eng., **2**(1): 53–63, 2008.
13. Kilani M.I., *Computer aided design tools in the development of surface micro-machined mechanisms*, Jordan J. Mech. Indust. Eng., **5**(2): 167–176, 2011.
14. Ding W.M., *Agricultural machinery study*, China Agricultural Press, Beijing, 2013.

Received September 29, 2016; accepted version March 14, 2017.